NASA TECHNICAL NOTE

NASA TN D-3527

NASA TN D-3527

METALLOGRAPHIC STUDY OF DISPERSION-STRENGTHENED ALLOYS AFTER FAILURE IN STRESS RUPTURE

by Charles A. Hoffman and John W. Weeton

Lewis Research Center
Cleveland, Ohio

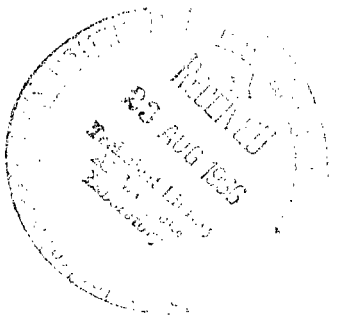

NATIONAL AERONAUTICS AND SPACE ADMINISTRATION • WASHINGTON, D. C. • AUGUST 1966

METALLOGRAPHIC STUDY OF DISPERSION-STRENGTHENED ALLOYS AFTER FAILURE IN STRESS RUPTURE

By Charles A. Hoffman and John W. Weeton

Lewis Research Center
Cleveland, Ohio

NATIONAL AERONAUTICS AND SPACE ADMINISTRATION

For sale by the Clearinghouse for Federal Scientific and Technical Information
Springfield, Virginia 22151 – Price $2.00

METALLOGRAPHIC STUDY OF DISPERSION-STRENGTHENED ALLOYS AFTER FAILURE IN STRESS RUPTURE

by Charles A. Hoffman and John W. Weeton

Lewis Research Center

SUMMARY

A metallographic study was conducted on stress-rupture failed specimens of a number of dispersion-strengthened materials to obtain additional insight into the microstructural factors affecting their stress-rupture strengths. This study led to the following conclusions: (a) in general, the dispersion strengthened materials investigated herein that exhibited best overall retention of stress-rupture strength had the most stable microstructures (i.e., these alloys had a superior resistance to porosity formation and/or particle coarsening), (b) those products which contained appreciable amounts of excess particles (i.e., measured volume fraction of dispersoid as compared with the nominal volume fraction of oxide) had good strength and stability at lower temperatures, but at higher temperatures their strengths decreased at a more rapid relative rate, and their microstructures exhibited increased porosity. The observed porosity is believed related to impurities, (c) there was no unique fracture mode that could be associated with those materials that retained a relatively greater portion of their stress-rupture strength at high temperatures, (d) the best overall retention of stress-rupture strength with increased use temperature was associated with materials having rather uniformly distributed dispersoid particles with fine characterizing dimensions ($<0.050\ \mu$), and (e) large particles, such as the $FeAl_3$ inclusions in an Al + 5 volume percent Al_2O_3 alloy, may be deleterious.

INTRODUCTION

Refractory particles, primarily oxides, have been used to dispersion strengthen various metallic matrices. In a number of instances, alloys of this type have been produced that have stress-rupture characteristics, particularly at longer times and higher temperatures, superior to comparable conventional alloys. A goal in these dispersion-

strengthened alloys is that the dispersoids resist dissolution and/or agglomeration at temperatures approaching the melting point of the matrix used. Dispersion-strengthened alloys have been made by utilizing techniques such as powder metallurgy, internal oxidation, or physicochemical methods involving colloidal techniques, or thermal decomposition of salts. Strain energy, which is believed to impart strength into this type of material, is generally introduced; this may be done by extruding or otherwise mechanically working the materials after initial compaction and/or sintering. Irmann (ref. 1) is well known for developing an aluminum plus alumina alloy that has unusually good high-temperature strengths and stability for an aluminum-base material. Subsequently, many investigators have attempted to obtain analogous high-temperature properties with other base metals; however, a good many of these products have not achieved high-temperature strength properties analogous to those of the aluminum plus alumina dispersion-strengthened material.

Although fundamental and applied studies of dispersion-strengthened products have been made by many investigators, further research appears necessary to explain better the properties of some of these products. In view of the foregoing, it was felt that a metallographic investigation of some dispersion-strengthened materials exhibiting unusually good or interesting stress-rupture properties could provide additional understanding of this type of material. The specific objectives of this particular investigation, which included a number of different dispersion-strengthened alloy systems and fabrication methods were as follows: (a) to determine whether or not a high degree of microstructural stability is necessarily associated with good stress-rupture strength and/or retention of this strength with increasing temperature (strength stability), (b) to determine whether any unique fracture mode (modes) may be associated with good stress-rupture strength and/or strength stability, and (c) to gain further understanding of the relative importance of microstructural parameters such as volume percent of oxide, particle size, and interparticle spacing in affecting stress-rupture strength and/or strength stability.

This study involved optical- and electron-microscopy investigations of failed stress-rupture specimens of aluminum-, copper-, or nickel-base materials to which were added either alumina or thoria. A large number of the materials investigated were obtained through the courtesy of other investigators. Some materials were obtained commercially. Stress-rupture tests were run at the Lewis Research Center on these latter materials. Microstructural studies were also made of nickel plus thoria materials subjected only to annealing at high temperature to obtain an indication of their thermal-microstructural stabilities.

MATERIALS, APPARATUS, AND PROCEDURE

Materials

The materials investigated included a number of compositions that exhibited unusually good or interesting stress-rupture properties, as indicated by a literature survey. Published stress-rupture properties (plotted herein as stress for rupture in 100 hours against homologous temperature) are shown for these materials in figure 1. Two commercially obtained material compositions were stress-rupture tested at the Lewis Research Center. Salient features of fabrication for all materials studied are listed in table I. The initial source of the materials (i.e., including original investigators) and condition upon receipt

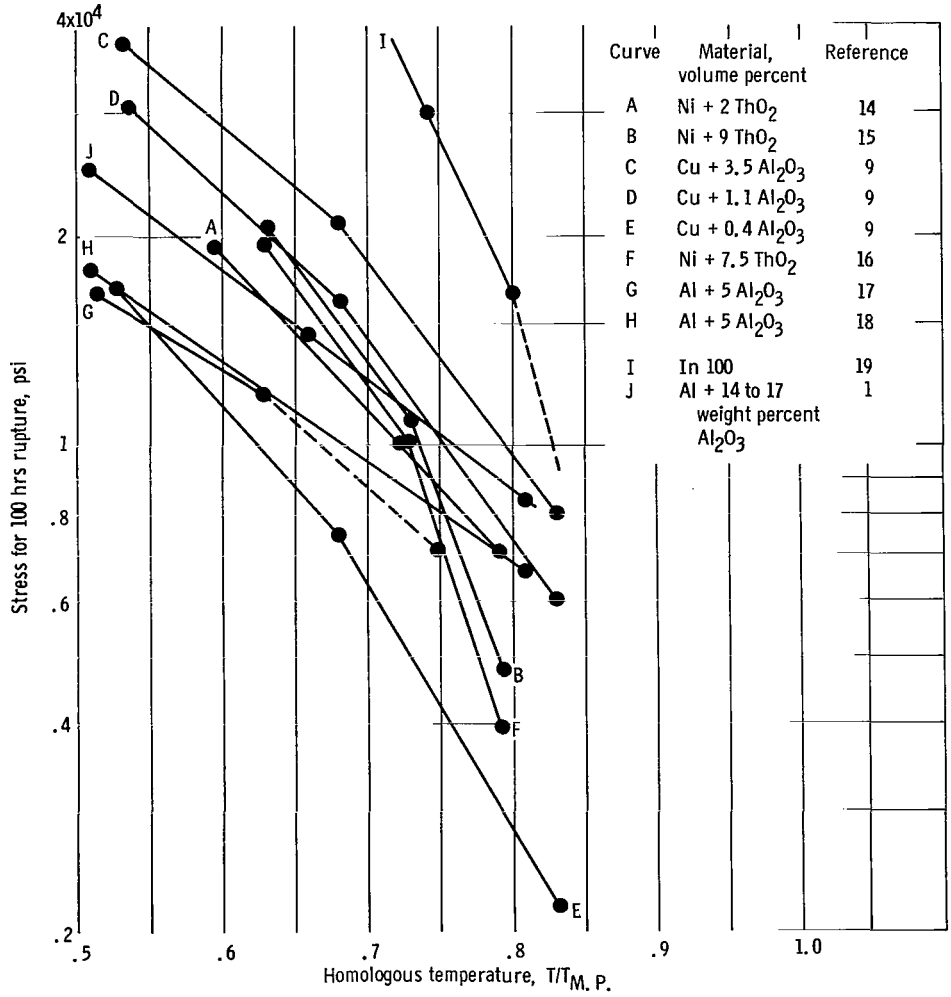

Figure 1. - One hundred hour creep-rupture stress as function of homologous temperature for selected dispersion strengthened alloys. Melting points of matrices: aluminum, 1190° F; copper, 1980° F; nickel, 2660° F. Data were taken from curves of stress against time to rupture at constant temperature. (A high-strength wrought nickel-base alloy (In 100) is included for comparison.)

TABLE I. - FABRICATION HISTORY OF SPECIMENS STUDIED

Material	Fabrication
Al + 5 volume percent Al_2O_3	Mechanical mixture of powders (ref. 17).
Cu + 3.5 volume percent Al_2O_3 Cu + 1.1 volume percent Al_2O_3 Cu + 0.4 volume percent Al_2O_3	Dispersion made by internally oxidizing chips of a dilute copper-aluminum alloy at 450° F with a subsequent diffusion treatment at 950° C (ref. 9).
Ni + 9 volume percent ThO_2	Nickel powder and thorium nitrate were dissolved in methyl alcohol. The slurry was dried and compacted, then heated in dry hydrogen to decompose the nitrate forming thoria on the nickel powder and also reducing any nickel monoxide (ref. 15).
Ni + 7.5 volume percent ThO_2	Dispersion made by mechanically mixing nickel and thoria. The thoria was produced by the precipitation of submicron thorium oxalate, which in turn was made from a concentrated thorium nitrate solution by the addition of saturated oxalic acid solution. The oxalate was washed, centrifuged, dried, and thermally decomposed to thoria by calcining; then it was ball-milled to bring it down to a submicron particle size. The metal-metal oxide mixture was hydrogen reduced to remove any nickel monoxide (ref. 16).
Ni + 2 volume percent ThO_2	Dispersion was made by using colloidal techniques wherein a nickel salt was deposited about thoria particles; the nickel salt was then reduced to pure nickel.

are given in table II. The materials furnished by Professor Nicholas J. Grant and coworkers (table II) were stress-rupture tested specimens.

Apparatus and Procedure

Conventional lever-type stress-rupture machines were used in conducting the stress-rupture tests at the Lewis Research Center. All fractured stress-rupture specimens were first examined macroscopically. Stress-rupture specimens were then mounted to obtain longitudinal sections through the fracture surface. These specimens were examined by using optical microscopy and photographed at magnifications up to X750. Specimens were then examined and photographed at up to X30 000 by using an electron microscope.

As-received material, which was available for the Al + 5 volume percent Al_2O_3 and

TABLE II. - SOURCE OF MATERIALS

Specimen	Material	Source	Condition	Stress-rupture tested at	Initial investigators
1	Al + 5 volume percent Al_2O_3	Alcoa	Rod	Lewis Research Center	----------
2	Cu + 3.5 volume percent Al_2O_3	Massachusetts Institute of Technology	Stress-rupture failed specimens	Massachusetts Institute of Technology	Preston and Grant (ref. 9)
3	Cu + 1.1 volume percent Al_2O_3	↓	↓	↓	Preston and Grant (ref. 9)
4	Cu + 0.4 volume percent Al_2O_3				Preston and Grant (ref. 9)
5	Ni + 9 volume percent ThO_2				Murphy and Grant (ref. 15)
6	Ni + 7.5 volume percent ThO_2				Predecki and Grant (ref. 16)
7	Ni + 2 volume percent ThO_2	Du Pont	Rod	Lewis Research Center	----------

Ni + 2 volume percent ThO_2 (Du Pont TD-Ni) materials, were examined metallographically.

Heat-treated specimens of Ni + 7.5 volume percent ThO_2 and of Ni + 2 volume percent ThO_2 were examined for the possible effects of thermal treatment alone on metallurgical stability. The former material was taken from the threaded end of a specimen already having been run for 37 hours at 1500° F in stress-rupture. This material was then heat treated for an additional 5 hours at 2000° F in a vacuum of 5×10^{-5} millimeter of mercury. The latter material, without any previous stress-rupture history, was thermally treated at 2000° F for 100 hours in high-purity argon.

The Al + 5 volume percent Al_2O_3 and the Ni + 2 volume percent ThO_2 alloys that were run in stress-rupture at this laboratory had, in most instances, a contoured gage section (i.e., hour glass configuration) such that failure was induced at the minimum cross section, in order to avoid radius failures that were encountered with the first few specimens of Al + 5 volume percent Al_2O_3 tested. Consequently all remaining stress-rupture tests of these two materials were run using the contoured design. The other specimens investigated had a uniform-diameter gage length. The contoured test specimen tended to localize the more severe microstructural effects within the region of minimum cross section.

Determination of Particle Parameters

The parameters (i. e., volume percent of particles, interparticle spacing, and particle size) were determined by using measurements taken from electron micrographs. Representative electron micrographs were selected and area analyses were made of them. A Zeiss-Endter particle size analyzer was used to determine the numbers of particles of given diameters in each electron micrograph. The area of each particle counted was visually equated to a circle of light, of comparable area, produced by the counter. For each micrograph, the total area occupied by the particles was determined after the number of particles of given diameters were obtained. The volume fraction of particles was taken as the ratio of the total particle area to the total area scanned.

The average particle sizes and interparticle spacings were calculated by using the following equations. These equations are slight modifications of those derived in reference 2, which in turn, were based in part on topological concepts derived in reference 3:

$$\overline{IPS} = \pi \frac{A}{P} \left(\frac{1}{f_{ox}} - 1 \right)$$

and

$$\overline{Z} = \pi \frac{A}{P}$$

where

$\overline{IPS}$ average interparticle spacing of particles in a three-dimensional array

A total particle area determined from micrograph (assuming circular plane sections for particles)

P total particle perimeter determined from micrograph (assuming circular plane sections for particles)

f_{ox} volume fraction of secondary phase particles (area of particle phase divided by total area scanned)

$\overline{Z}$ average particle intercept dimension, defined as the average intercepted length on randomly oriented straight lines through a random three-dimensional array of particles

RESULTS

Stress-Rupture Studies

The stress-rupture results obtained at the Lewis Research Center on the Al + 5 vol-

TABLE III. - STRESS-RUPTURE RESULTS

Material	Specimen	Test temperature, °F	Homologous temperature, $T/T_{M.P.}$	Stress-rupture test atmosphere	Specimen stress, psi	Time to rupture, hr
Al + 5 volume percent Al_2O_3	1-1	800	0.74	Air	10 000	0.05
	1-2	800	.74	Air	7 000	4.80
	1-3	800	.74	Air	7 000	11.70
	1-4	800	.74	Air	6 000	165.00
	1-5	800	.74	Air	(a)	3609.50
Cu + 3.5 volume percent Al_2O_3	2-1	1202	0.675	Air	22 500	39.10
Cu + 1.1 volume percent Al_2O_3	3-1	1202	0.675	Air	26 000	0.04
	3-2	1202	.675	Air	15 000	234.00
	3-3	1562	.82	Nitrogen	12 500	.10
Cu + 0.4 volume percent Al_2O_3	4-1	1562	0.82	Nitrogen	6 500	0.09
Ni + 9 volume percent ThO_2	5-1	1500	0.635	Air	27 000	0.30
	5-2	1500	.635	Air	21 000	91.00
	5-3	2000	.80	Air	15 000	.02
	5-4	2000	.80	Air	7 000	6.00
Ni + 7.5 volume percent ThO_2	6-1	1500	0.635	Air	18 000	37.00
	6-2	2000	.80	Nitrogen	13 000	.09
	6-3	2000	.80	Nitrogen	7 500	4.80
Ni + 2 volume percent ThO_2	7-1	1800	0.73	Air	20 000	(b)
	7-2	1800	.73	Air	15 000	0.30
	7-3	1800	.73	Air	12 000	107.00
	7-4	1800	.73	Air	10 000	1868.40

[a]Stress increased at this time from 5000 to 10 000 psi and specimen fractured immediately.

[b]Failed on loading.

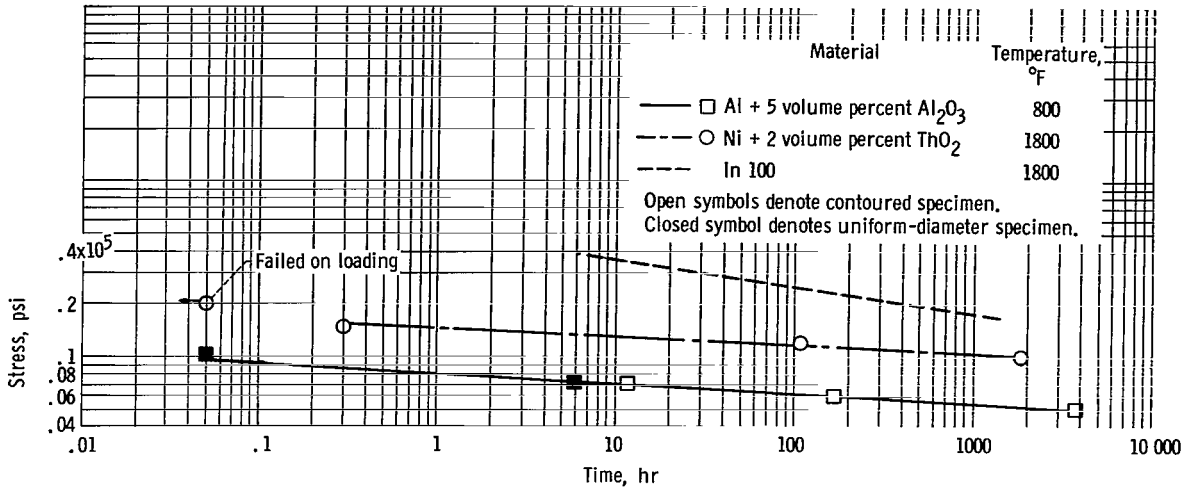

Figure 2. - Stress-rupture lives of materials tested at Lewis Research Center.

ume percent Al_2O_3 and the Ni + 2 volume percent ThO_2 materials are included in table III and are plotted in figure 2.

Note that the slopes of the stress-rupture curves for the Ni + 2 volume percent ThO_2 and the Al + 5 volume percent Al_2O_3 materials were almost identical. This similarity should not be surprising considering the fact that the test temperatures for the two different materials were approximately the same on a homologous scale: namely, 73 percent for the nickel plus thoria material and 74 percent for the aluminum plus alumina oxide material (1800° and 800° F, respectively). It was mentioned in the preceding section that the aluminum plus alumina specimens were tested in both contoured and in the uniform-diameter conditions and that there was essentially no difference between the properties of the two as may be seen in this figure. The other data presented in table III were generated by the respective investigators listed in table II.

Metallographic Studies

For ease of reference, a list of all specimens metallographically studied is presented in table IV. Included in this table is a list of conditions of materials prior to metallographic examination, the type of microscopy utilized, and the respective figure numbers.

As-received materials were available for microstructural study for the two alloys, Al + 5 volume percent Al_2O_3 and Ni + 2 volume percent ThO_2. Photomicrographs are presented in figures 3(a) and (b) that are representative of Al + 5 volume percent Al_2O_3 and Ni + 2 volume percent ThO_2, respectively. In the case of the former material a large gray phase may be noted, which was identified as $FeAl_3$ with the aid of the electron

TABLE IV. - CONDITION OF MATERIALS STUDIED METALLOGRAPHICALLY

Specimen	Shown in fig. -	Material	Condition of specimens prior to metallographic study			Type of microscopy		
			As received	Stress-rupture tested	Stability heat treated	Macro-optical	Micro-optical	Electron
---	3(a)	Al + 5 volume percent Al_2O_3	✓				✓	
1-1	4(a)			✓		✓		
1-4	4(b)			✓		✓		
1-5	4(c)			✓		✓		
1-1	6(a)			✓			✓	
1-3	6(b)			✓			✓	
1-4	6(c)			✓			✓	
1-5	6(d), (e)			✓			✓	
---	6(f)			✓				✓
2-1	7(a), (b)	Cu + 3.5 volume percent Al_2O_3		✓			✓	
2-1	8(a), 9(a)			✓				✓
3-2	4(d)	Cu + 1.1 volume percent Al_2O_3		✓		✓		
3-3	7(c)			✓			✓	
3-2	8(b), 9(b), (c), 10(a)			✓				✓
3-3	9(d)			✓				✓
4-1	8(c), 9(e), 10(b)	Cu + 0.4 volume percent Al_2O_3		✓				✓
5-4	4(e)	Ni + 9 volume percent ThO_2		✓		✓		
5-2	11(a)			✓			✓	
5-4	11(b), (c)			✓			✓	
5-4	11(d)			✓				✓
6-1	14(a)	Ni + 7.5 volume percent ThO_2		✓			✓	
6-1	14(b)				✓[a]		✓	
6-1	14(c)				✓[a]			✓
6-1	11(e)			✓				✓
6-3	11(f)			✓				✓
---	3(b)	Ni + 2 volume percent ThO_2	✓					
---	15(a)		✓					
7-4	4(f)			✓		✓		
7-2	12(a)			✓		✓		
7-4	12(b), (c)			✓		✓		
7-4	13(a), (b), (c)			✓				✓
---	15(b)				✓			

[a]Stability annealed subsequent to 37 hr at 1500° F in stress rupture.

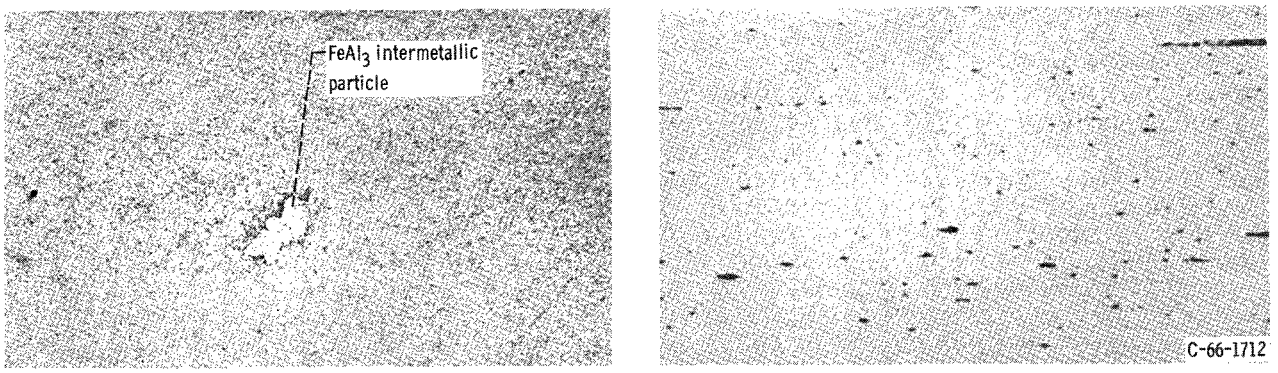

(a) Al + 5 volume percent Al_2O_3. X250.

(b) Ni + 2 volume percent ThO_2. X750.

Figure 3. - Photomicrographs of longitudinal cross section of as received and polished Al + 5 volume percent Al_2O_3 and Ni + 2 volume percent ThO_2 alloys obtained from commercial sources.

TABLE V. - FRACTURE SURFACE OBSERVATIONS

Material	Specimen	Macrofracture surface characteristics
Al + 5 volume percent Al_2O_3	1-1	Cup and cone
	1-2	Cup and cone
	1-3	Brittle appearance with granular texture
	1-4	Brittle appearance with granular texture
	[a]1-5	Shear (along 45° plane)
Cu + 3.5 volume percent Al_2O_3	2-1	Ductile with shear facets
Cu + 1.1 volume percent Al_2O_3	3-1	Ductile with shear facets
	3-2	Ductile with shear facets
	3-3	Ductile with shear facets
Cu + 0.4 volume percent Al_2O_3	4-1	Ductile with shear facets
Ni + 9 volume percent ThO_2	5-1	Brittle with course granular texture
	5-2	↓
	5-3	
	5-4	
Ni + 7.5 volume percent ThO_2	6-1	Brittle with course granular texture
	6-2	Brittle with course granular texture
	6-3	Brittle with course granular texture
Ni + 2 volume percent ThO_2	7-1	Brittle with course granular texture
	7-2	Brittle with course granular texture
	7-3	Brittle with course granular texture
	7-4	Brittle with fine granular texture

[a]Specimen ran for 3609.5 hr at 5000 psi at which time the stress was increased to 10 000 psi and immediate fracture occurred.

microprobe. Inclusions of $FeAl_3$ have also been observed in aluminum (sintered aluminum powder) by other investigators (refs. 4 and 5). Specimens of the latter material had a wrought structure, and the specimen axis was made parallel to the fibrous structure.

Macrofracture Characteristics of Typical Stress-Rupture Tested Specimens of All Alloys

The macroscopic fracture appearance of the various specimens studied are summarized in table V. There is a considerable difference in the fracture appearance of the different types of dispersion-strengthened materials. Because some of these features are felt to warrant further description, each alloy will be described individually.

Aluminum plus 5 volume percent alumina. - The macrofracture characteristics of Al + 5 volume percent Al_2O_3 specimens are shown in figures 4(a) to (c). The specimen shown in figure 4(a) failed in 0.05 hour and is similar in appearance to one having failed

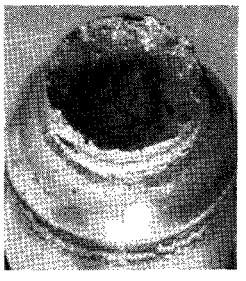

(a) Al + 5 volume percent Al_2O_3 tested for 0.05 hour at 800° F. Specimen exhibited cup and cone fracture.

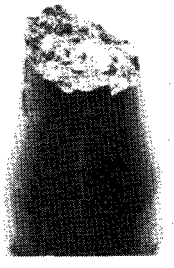

(b) Al + 5 volume percent Al_2O_3 tested for 165 hours at 800° F. Specimen exhibited brittle fracture with granular texture.

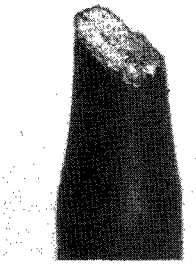

(c) Al + 5 volume percent Al_2O_3 tested for 3609.5 hours at 800° F. Specimen exhibited ductile fracture (gross 45° shear).

(d) Cu + 1.1 volume percent Al_2O_3 tested for 0.1 hour at 1202° F. Specimen exhibited ductile fracture with pronounced shear facets.

(e) Ni + 9 volume percent ThO_2 tested for 6 hours at 2000° F. Specimen exhibited brittle fracture with coarse granular texture.

(f) Ni + 2 volume percent ThO_2 tested for 1868.4 hours at 1800° F. Specimen exhibited brittle fracture with fine granular texture.

Figure 4. - Typical macrophotographs of stress-rupture failed specimens showing different types of fracture surfaces. X3.

after 4.8 hours; they both exhibited cup and cone fractures. These fractures occurred at the radii leading into the test section. Because of the location of these fractures, the specimen was redesigned to make the transition into the test section more gradual and to cause fracture to occur in the center of the test zone rather than at the shoulder, as was discussed in the Apparatus and Procedure section.

The specimens shown in figures 4(b) and (c) were of the modified design. The specimen shown in figure 4(b) ran for 165 hours at a stress of 6000 pounds per square inch and exhibited a granular appearing surface that appeared to consist of numerous shear facets. A specimen that failed at 11.7 hours (specimen 1-3, table III) exhibited a similar fracture surface; therefore the photograph is not shown. The specimen shown in figure 4(c) ran for 3609.5 hours at a stress of 5000 pounds per square inch at which time the load was raised to 10 000 pounds per square inch and the specimen failed immediately along a gross plane essentially at 45° to the specimen axis.

Copper plus 3.5, 1.1, and 0.4 volume percent alumina. - All specimens of these three compositions had essentially the same type of macrofracture surface appearance. The specimen shown in figure 4(d) is typical of these specimens and shows numerous pronounced shear facets.

Nickel plus 9 and 7.5 volume percent thoria. - A macrograph of a typical specimen of one of these compositions is shown in figure 4(e). The fractures were essentially normal to the specimen axis, appeared brittle, and had a coarse granular texture.

Nickel plus 2 volume percent thoria. - A macrograph of a typical specimen of this material is presented in figure 4(f). The fracture surface was essentially transverse to the specimen axis, and the surface had an unusually fine granular texture and a slight shear lip. The shorter time specimens of this composition manifested a coarser granular fracture surface texture.

Particle Parameter Measurements

The measured volume percents of oxide, the particle sizes (i.e., average intercept) and average interparticle spacings are summarized in table VI. In addition, the uniformities of particle distribution are also described.

For Al + 5 volume percent Al_2O_3, the measured volume fractions of particles were in good agreement with the nominal amounts. Caution has to be exercised in the etching of dispersion-strengthened materials, particularly the Al + 5 volume percent Al_2O_3. Over etching tends to give an indication of an overly large volume fraction of oxide, and as a consequence will also result in an erroneously small interparticle spacing.

For two of the three copper plus alumina products (i.e., nominal 1.1 and 0.4 volume percent Al_2O_3) the observed volume percents of fine background oxide (over and above

TABLE VI. - DISPERSOID PARTICLE MEASUREMENTS

[Measurements based on longitudinal cross sections.]

Specimen	Material	Condition of specimen	Volume of particle, percent	Interparticle spacing, μ	Intercept particle size, μ	Particle shape and distribution
1	Al + 5 volume percent Al_2O_3	As received	5.9	2.3	[a]0.14	Uniformly distributed flakes
2		As received	4.2	2.1	[a].09	
3		Tested for 3609.5 hr at 800° F	8.0	1.3	[a].15	
4		Tested for 3609.5 hr at 800° F	6.6	2.4	[a].17	
5	Cu + 3.5 volume percent Al_2O_3	Tested for 39.1 hr at 1202° F	[b]2.0	[b]1.3	[b]0.03	Uniformly distributed spherical fine background particles; with bands of large particles
6	Cu + 1.1 volume percent Al_2O_3	Tested for 234 hr at 1202° F	[b]2.4	[b]1.9	[b].05	
7	Cu + 0.4 volume percent Al_2O_3	Tested for 0.09 hr at 1562° F	[b]4.5	[b]1.5	[b].05	
8	Ni + 9 volume percent ThO_2	Tested for 0.3 hr at 1500° F	19	1.2	0.29	Slightly banded spherical particles
9		Tested for 6 hr at 2000° F	12	1.6	.21	
10	Ni + 7.5 volume percent ThO_2	Tested for 37 hr at 1500° F	19	0.84	0.20	Slightly banded spherical particles
11		Tested for 4.5 hr at 2000° F	15	1.1	.21	
12	Ni + 2 volume percent ThO_2	As received	2.5	1.8	0.05	Uniformly distributed spherical particles
13		Tested for 1868.4 hr at 1800° F	3.0	1.7	.05	

[a]Particle thickness reported to be 0.005μ to 0.05μ in literature (refs. 7 and 8).
[b]Based on background particles only.

the banded coarse particles) were 2.4 and 4.5 which were approximately 2 and 11 times greater than the respective nominal amounts. In fact, the measured volume percent of particles appeared to be inversely related to the nominal values of oxide for the three copper plus alumina products studied.

For the Ni + 9 volume percent ThO_2 specimen tested at the lower temperature and for a relatively short time before failure, the measured volume percent of particle (i.e., 19 percent) was considerably greater (by a factor of about 2) than the nominal amount of

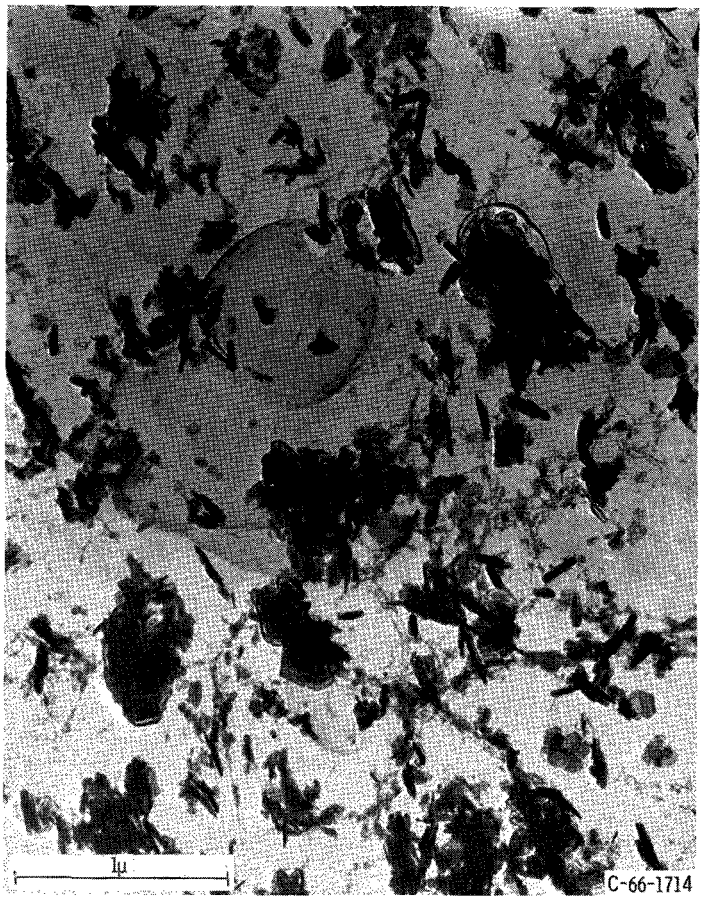

Figure 5. - Electron micrograph of aluminum oxide particles extracted from an Al + 5 volume percent Al_2O_3 alloy. X46 000.

thoria. The specimen given a more severe test exposure had a smaller amount of measured dispersoids, namely 12 percent. This observation also pertains to the Ni + 7.5 volume percent ThO_2 product.

For the Ni + 2 volume percent ThO_2 alloy, the measured amount of particle was similar to the nominal amount of thoria. Furthermore, the quantity measured appeared to have been unaffected by stress-rupture exposure.

The interparticle spacing measurements were of the order of 1 to 2 microns for all the specimens examined. Study of particle sizes revealed that the Cu + Al_2O_3 and the Ni + 2 volume percent ThO_2 materials were on the order of 0.03 to 0.05 micron. The other products had particle sizes of about 0.1 to 0.3 micron.

For Al + 5 volume percent Al_2O_3, the oxide particles appeared to be platelets, as may be seen from figure 5. In reference 6, it is postulated that the dispersed-phase particle thickness is of great importance in influencing the strength of aluminum alloys. This postulate is believed to be reasonable, and hence the platelet thickness rather than an average intercept dimension should be used to characterize the size of these particles.

In line with this postulate, the characterizing dimension for the alumina particles was assumed to be in the range 0.005 (ref. 7) to 0.05 micron (ref. 8).

With regard to uniformity of oxide particle distribution, the Al + 5 volume percent Al_2O_3 and the Ni + 2 volume percent ThO_2 products have good uniformity; the copper plus alumina products have uniform "fine" background particles, but in addition have bands of coarser particles. These coarser particles are about an order of magnitude larger than the fine background dispersoids. The Ni + 7.5 volume percent ThO_2 and Ni + 9 volume percent ThO_2 materials have a tendency toward banded, as well as somewhat elongated oxide particles.

Microstructures of Failed Stress-Rupture Specimens

Aluminum plus 5 volume percent alumina. - Figure 6(a) shows the microstructure of the side of a cup and cone fracture previously referred to in connection with specimens of this material shown in figure 4. The fracture path is approximately 45° to the specimen axis along the side. The specimens shown in figures 6(b) and (c) exhibit what appear to be numerous shear facets along the fracture surface. This fracture appearance was typical of the specimens run in stress-rupture for intermediate times. For the specimen that ran for a total of 3609.5 hours, the fracture path is seen to be at essentially 45° to the specimen axis (fig. 6(e)); however, it should be recalled that this specimen was run for 3609.5 hours at 5000 pounds per square inch at which time the stress was doubled causing immediate failure to occur. Hence, the fracture of this particular specimen is not necessarily typical of that to be expected in longtime stress-rupture, but probably represents the combined effects of both low- and high-strain rate exposure.

For all the aluminum plus alumina specimens, cracking or porosity formation appears to be associated with the $FeAl_3$ intermetallic phase particles. These intermetallic particles were several orders of magnitude larger than the intercept size of the background dispersoids. In the case of the specimen of this material shown in figure 6(a), an $FeAl_3$ intermetallic particle fractured, which caused a crack to propagate into the matrix. For another specimen (fig. 6(c)), cracking also appeared to proceed from intermetallic particles, and in addition porosity appeared adjacent to the intermetallic particles. Note that there was no appreciable surface oxidation or auxiliary surface cracking in any of the Al + 5 volume percent Al_2O_3 specimens. At optical microscopy magnifications, stress-rupture specimens of this material were relatively unaffected at locations below the fracture surface (figs. 6(a) to (e)) except for the cracks within and the pores adjacent to the $FeAl_3$ intermetallic phase particles. In the case of the as-received material (fig. 3(a)) no cracks or pores were noted to be associated with the intermetallic phase particles.

The only defect revealed by electron microscopy of the specimen shown in figure

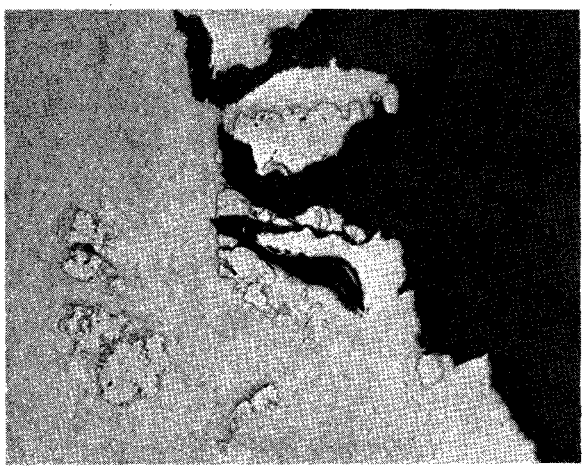

(a) Tested for 0.05 hour at 800° F. X250.

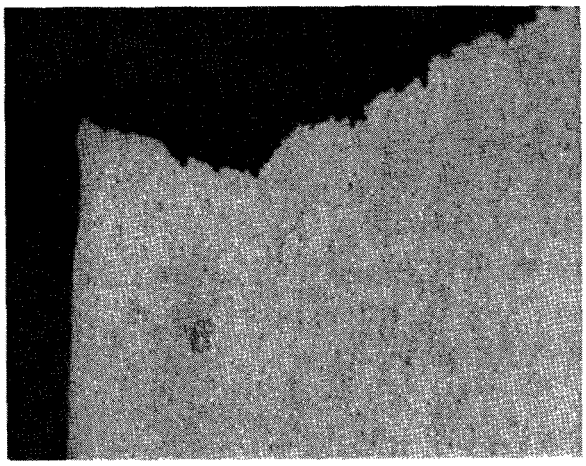

(b) Tested for 11.7 hours at 800° F. X250.

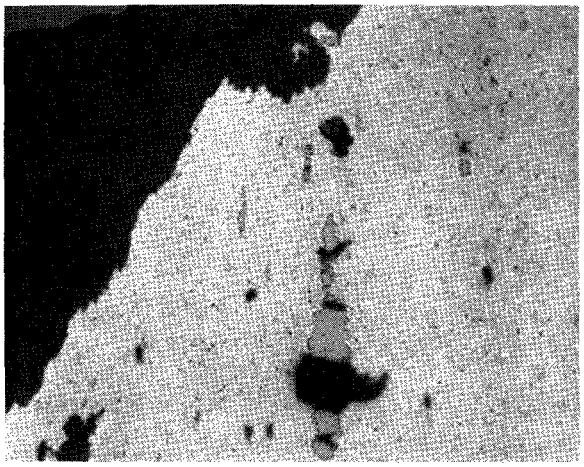

(c) Tested for 165.0 hours at 800° F. X250.

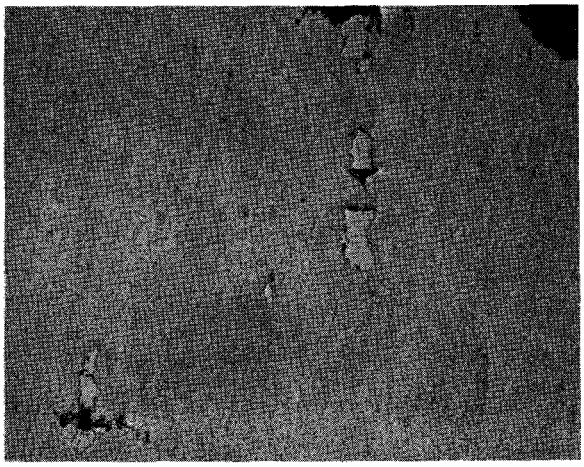

(d) Tested for 3605.5 hours at 800° F. X250.

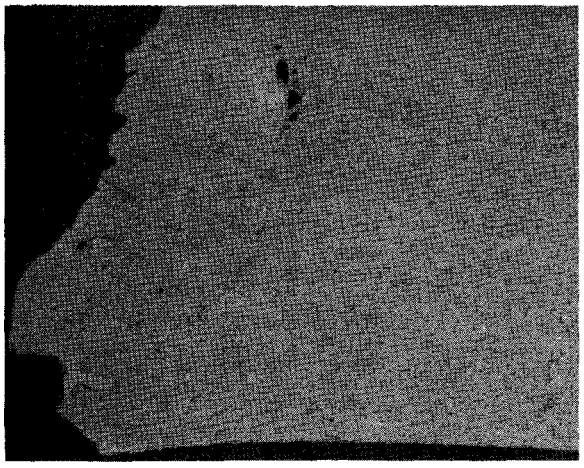

(e) Tested for 3609.5 hours at 800° F. X250.

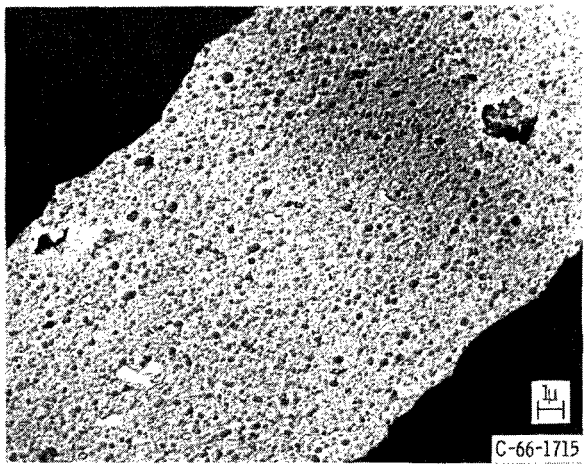

(f) Replication electron micrograph. Tested for 3609.5 hours at 800° F. X7000.

Figure 6. - Microstructures of an as-polished Al + 5 volume percent Al_2O_3 alloy after failure by stress rupture. (Note the general stability of microstructure and cracking within and porosity formation adjacent to intermetallic $FeAl_3$ particles.)

6(f), which was run for 3609.5 hours, was a small amount of porosity. A fine substructure (or perhaps a pitting effect) appeared to be present, and the voids or porosity that were observed were generally in the vicinity of the $FeAl_3$ intermetallic phase. The extraction replica shown in figure 5 was made to delineate more exactly the shape of the alumina particles since they were obscure in the replication electron micrographs. In the extraction micrograph, the oxide particles appeared to be twisted platelets.

Copper plus 3.5, 1.1, and 0.4 volume percent alumina. - The data of figure 7 verify and extend the observations made on the macrofracture surfaces of the copper plus alumina products, mainly that the prime fractures, as well as the microcracks, occurred by shear. In addition, the microstructure is seen to be banded. For Cu + 0.4 volume percent Al_2O_3, for which no micrograph is shown, the shear facets along the prime fracture surface were not very predominant. Stress-rupture testing of the copper plus alumina specimens is believed to have caused little, if any, microstructural damage compared

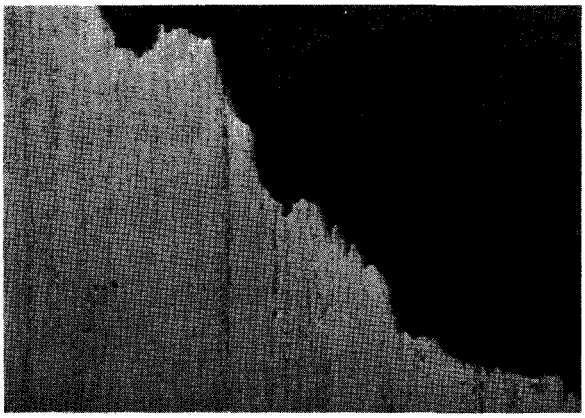

(a) Cu + 3.5 volume percent Al_2O_3 tested for 39.1 hours at 1202° F. As polished.

(b) Cu + 3.5 volume percent Al_2O_3 tested for 39.1 hours at 1202° F. Etched.

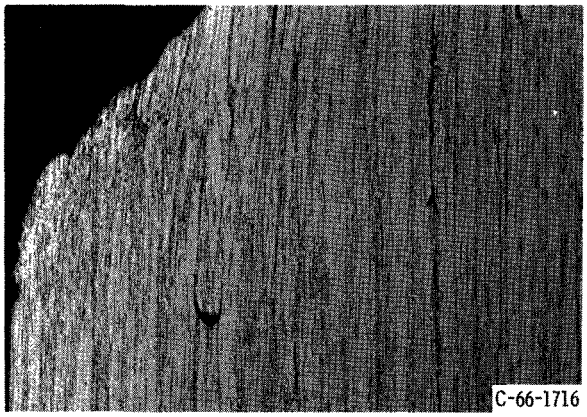

(c) Cu + 1.1 volume percent Al_2O_3 tested for 0.1 hour at 1562° F (nitrogen atmosphere). Etched.

Figure 7. - Typical microstructures of copper plus alumina specimens tested in stress-rupture. (Note the occurence of shearing and internal cracks and banding for particles.) X100.

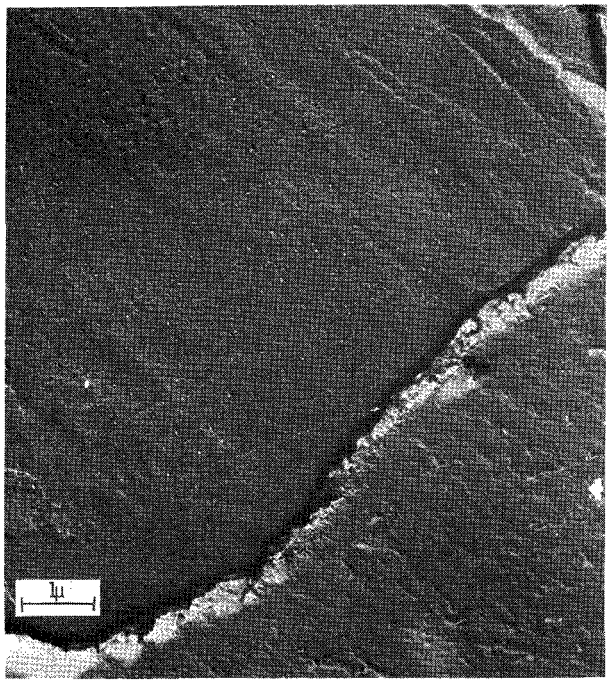

(a) Cu + 3.5 volume percent Al_2O_3 tested for 39.1 hours at 1202° F. X19 000.

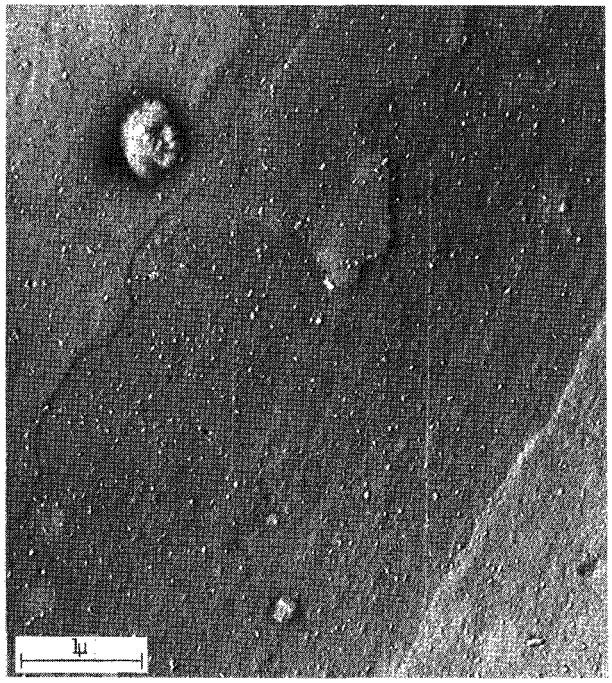

(b) Cu + 1.1 volume percent Al_2O_3 tested for 234 hours at 1202° F. X30 000.

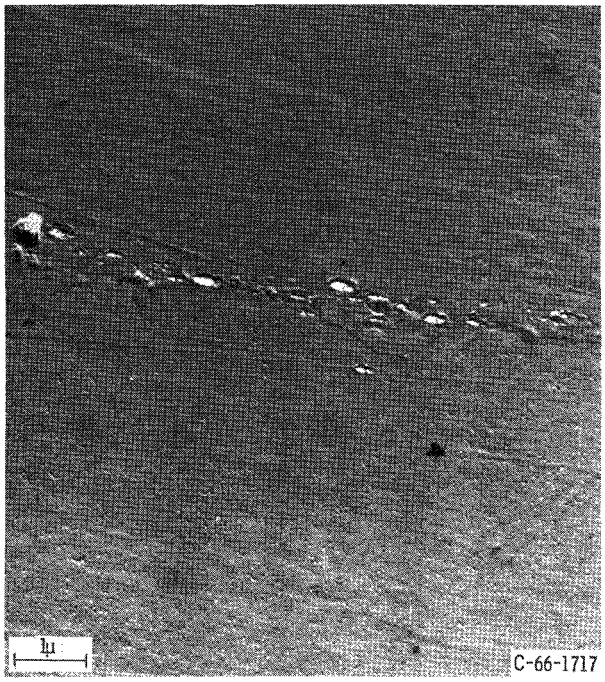

(c) Cu + 0.4 volume percent Al_2O_3 tested for 0.09 hour at 1562° F (nitrogen atmosphere). X19 000.

Figure 8. - Fine dispersoids observed in copper plus alumina materials.

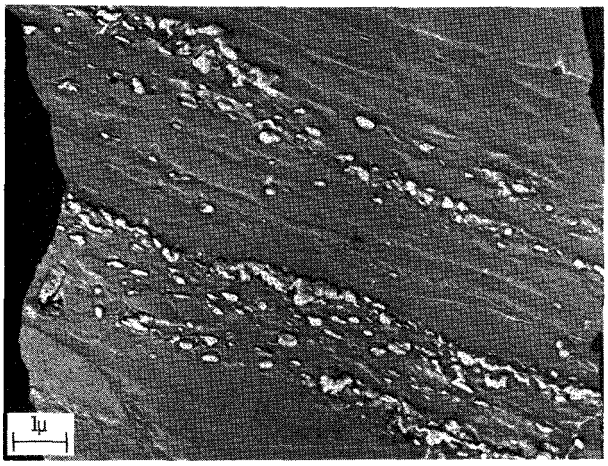

(a) Cu + 3.5 volume percent Al_2O_3 tested for 39.1 hours at 1202° F. X7000.

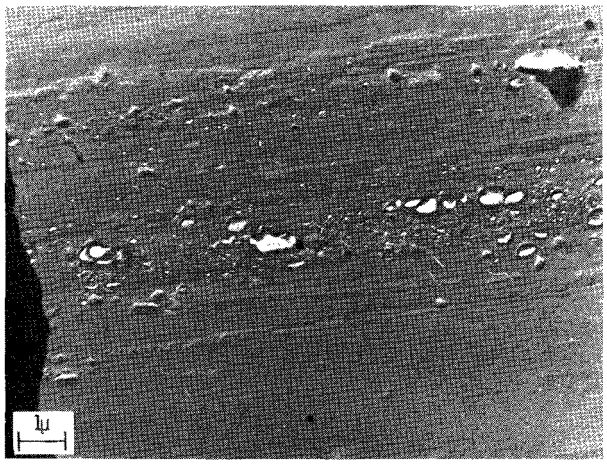

(b) Cu + 1.1 volume percent Al_2O_3 tested for 234 hours at 1202° F. (area 1). X7000.

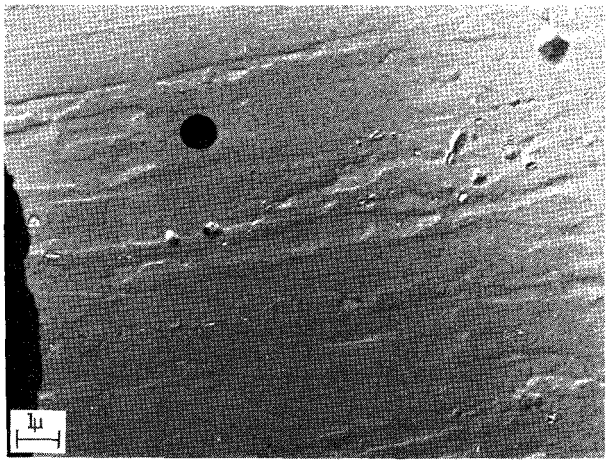

(c) Cu + 1.1 volume percent Al_2O_3 tested for 234 hours at 1202° F. (area 2). X7000.

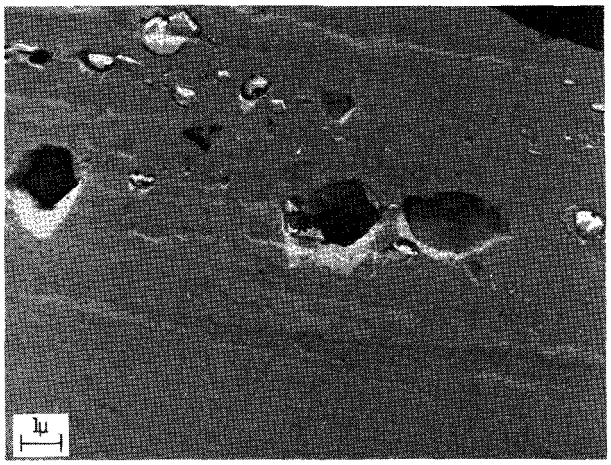

(d) Cu + 1.1 volume percent Al_2O_3 tested for 0.1 hour at 1562° F (nitrogen atmosphere). X10 000.

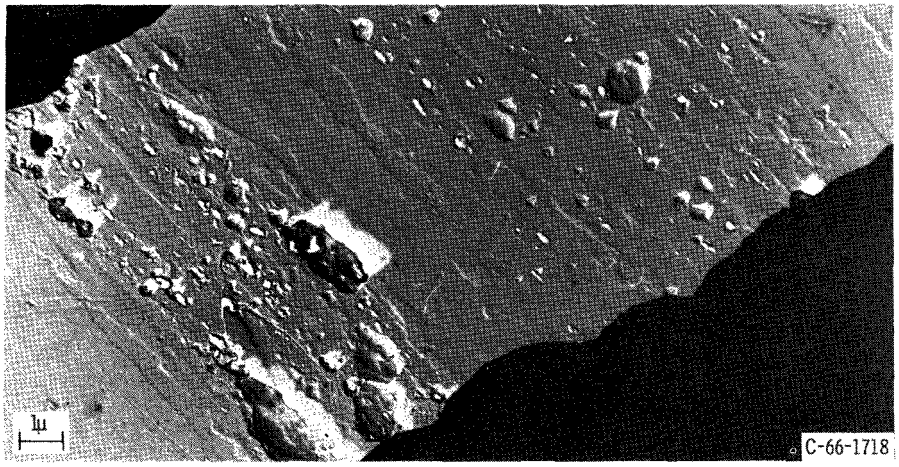

(e) Cu + 0.4 volume percent Al_2O_3 tested for 0.09 hour at 1562° F (nitrogen atmosphere). X7000.

Figure 9. - Copper plus alumina specimens exhibiting bands of coarse particles and increase in porosity with decreasing volume percent oxide and increasing temperature.

with the as-extruded structure, which is shown in figure 4 of reference 9. In some regions of the present specimens it appeared as though fibrous "bands" had necked down and ruptured (fig. 7(c)).

Electron micrographs of the copper-alumina specimens (figs. 8 and 9) revealed that this system had an exceedingly fine background precipitate (fig. 8) along with the bands of larger and somewhat stringered particles (fig. 9). Measurements of particle size and spacing presented earlier in table VI indicated that the directly measured size of the fine background precipitate in the Cu + 3.5 volume percent Al_2O_3 alloy were on the order of 0.03 micron with an interparticle spacing of 1.3 microns. Figures 8(a) and 9(a) show also that the structure for the Cu + 3.5 volume percent Al_2O_3 alloy remained relatively unchanged; for example, no pores or other major defects appeared to be produced by testing at 1202° F (650° C) or 0.67 $T/T_{M.P.}$ for 39.1 hours.

Values for the fine particles in the Cu + 1.1 volume percent Al_2O_3 alloy, based on measurements made on electron micrographs, are 0.05 and 1.9 microns (table VI), respectively, for size and spacing. Figure 9(d) reveals porosity in the vicinity of the coarser oxide bands of a specimen of Cu + 1.1 volume percent Al_2O_3 tested at 1562° F (850° C) or 0.82 $T/T_{M.P.}$; however, no appreciable porosity was evident in specimens

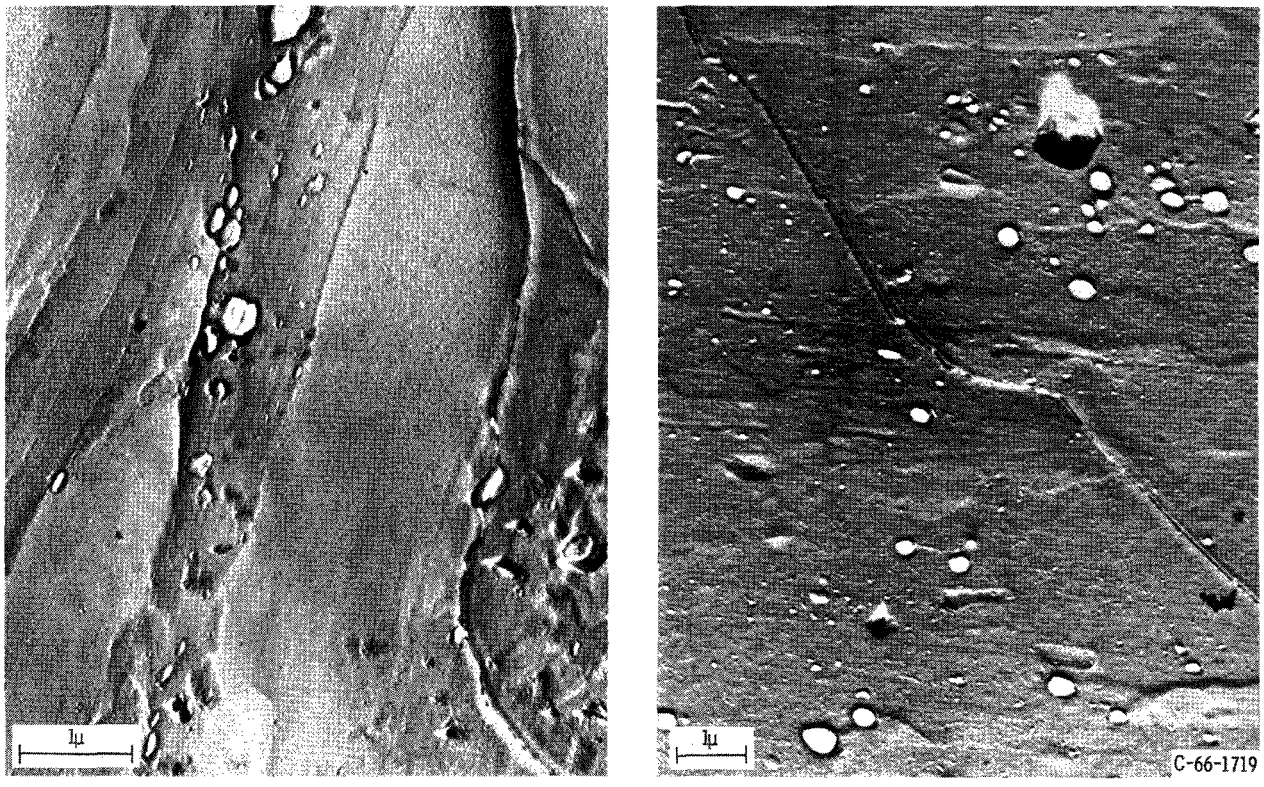

(a) Cu + 1.1 volume percent Al_2O_3 tested for 234 hours at 1202° F. X30 000.

(b) Cu + 0.4 volume percent Al_2O_3 tested for 0.09 hour at 1562° F. X19 000.

Figure 10. - Crack propagation in vicinity of larger particles in copper plus alumina specimens.

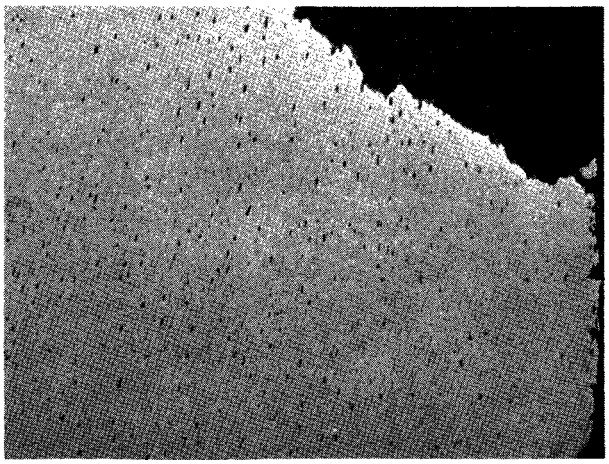

(a) As-polished Ni + 9 volume percent ThO_2 tested for 91 hours at 1500° F. X100.

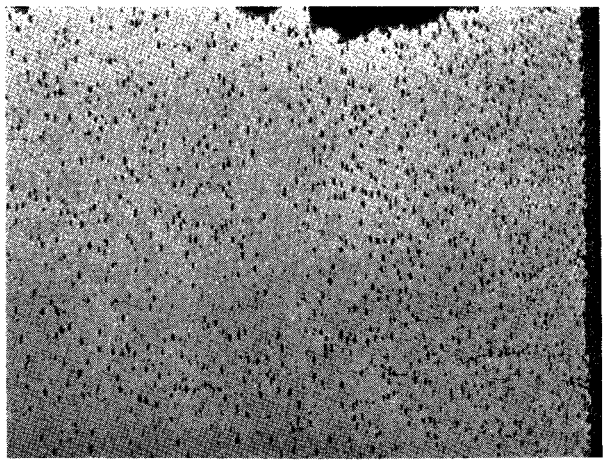

(b) As-polished Ni + 9 volume percent ThO_2 tested for 6 hours at 2000° F. X100.

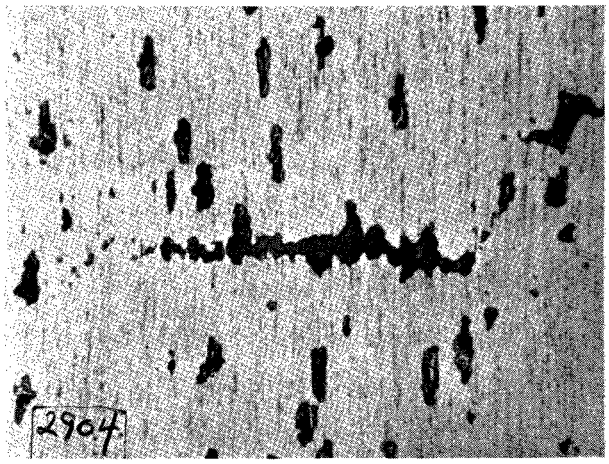

(c) As-polished Ni + 9 volume percent ThO_2 tested for 6 hours at 2000° F. X750.

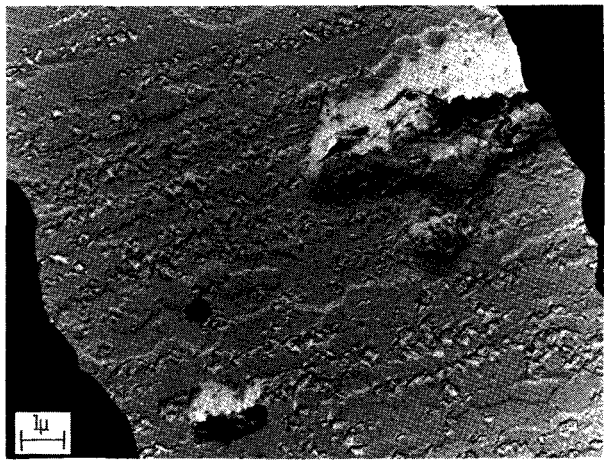

(d) Ni + 9 volume percent ThO_2 tested for 6 hours at 2000° F. X7000.

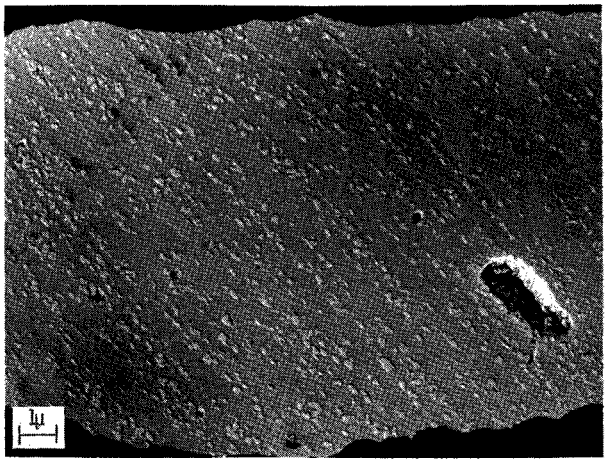

(e) Ni + 7.5 volume percent ThO_2 tested for 37 hours at 1500° F. X7000.

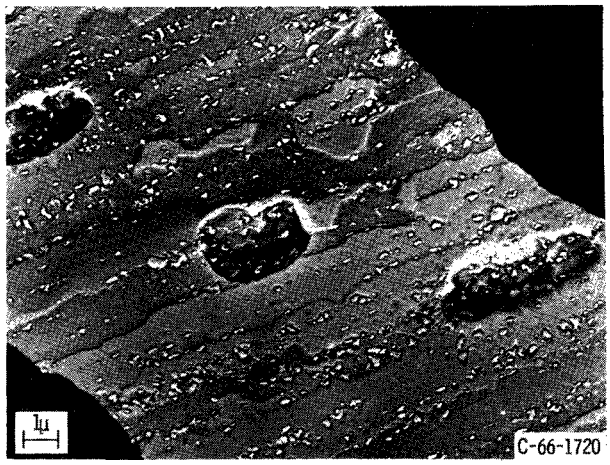

(f) Ni + 7.5 volume percent ThO_2 tested for 4.8 hours at 2000° F. X7000.

Figure 11. - Nickel plus high volume thoria specimens exhibiting increasing porosity with increasing stress-rupture temperature and also exhibiting incipient cracks due to linkup of pores.

run at 1202° F. Figure 10(a) shows microcracks that appeared to have propagated around oxide particles in their paths.

Parameters for the fine particles in the Cu + 0.4 volume percent Al_2O_3 alloy were determined in this study to be 0.05 micron for particle size and 1.5 micron for interparticle spacing (table VI). Extensive porosity may be observed in the vicinity of the bands of coarse oxide in the specimen shown in figure 9(e), which was run at 1562° F for only 0.09 hour. Figure 10(b) shows a shear crack that may have been deflected by particles in this particular specimen.

Nickel plus 9 volume percent thoria. - Typical fracture surfaces for this material are illustrated in the optical micrographs shown in figures 11(a) and (b). These fracture surfaces do not give clear indications of the fracture mode (modes). Specimens of this material revealed appreciable and progressively more extensive porosity formation as the stress-rupture temperature was increased (figs. 11(a) and (b)). For the specimen shown in figure 11(c), which ran for 6 hours at 2000° F, porosity formation with subsequent "linkup" of these regions was indicated. Surface oxidation of this material may be observed in figures 11(a) and (b).

An electron micrograph of a specimen (fig. 11(d)), which was stress-rupture tested for 6 hours at 2000° F (same specimen as shown in fig. 11(c)), reveals clustered particles as well as porosity. The small gray areas in the optical micrograph of figure 11(c) probably correspond to the clustered oxides seen in the electron micrograph, and the larger black areas found in the optical micrograph is the porosity observed in the electron micrograph.

Nickel plus 7.5 volume percent thoria. - The microstructures of the Ni + 7.5 and 9 volume percent ThO_2 materials after stress-rupture testing were similar. The same observations made for the Ni + 9 volume percent ThO_2 product also apply to the Ni + 7.5 volume percent material. The electron micrograph shown in figure 11(e) for a specimen of the Ni + 7.5 volume percent ThO_2 alloy, which was tested at a relatively low temperature and short time (1500° F for 37 hr) shows numerous small pores adjacent to particles, as well as some larger pores. A specimen of the same composition (fig. 11(f)) was exposed to a more severe stress-rupture condition of 4.8 hours at 2000° F. Numerous large pores as well as some small pores are exhibited. The grains of these two materials were very fine and highly elongated.

Nickel plus 2 volume percent thoria (DuPont Td-Nickel). - Microstructures of typical specimens are shown in figure 12. Observation of a specimen that ran for 0.3 hour at 1800° F (fig. 12(a)) indicated a possibility of the linkup of porosity. No gross structural changes were observed from the optical micrographs by comparing the as-received structure shown in figure 3(b) (p. 10) with the stress-rupture specimens in figure 12. Surface oxidation was noticed in stress-rupture tested specimens.

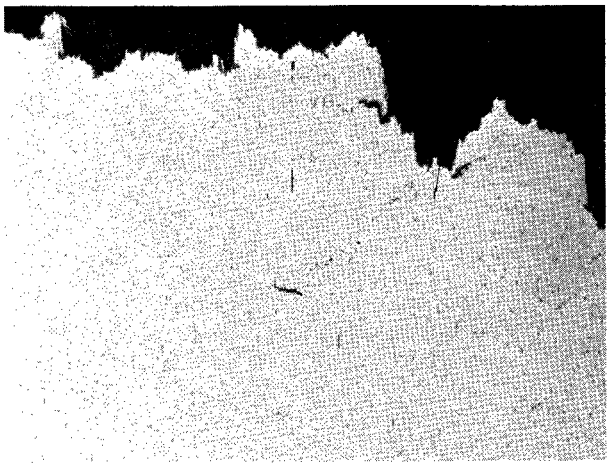

(a) Tested for 0.3 hour at 1800° F. X100.

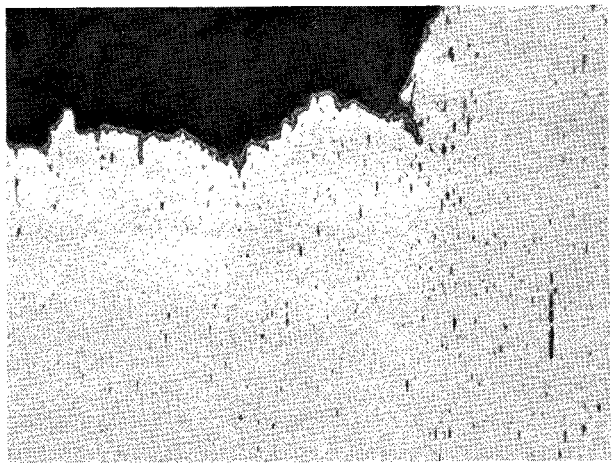

(b) Tested for 1868.4 hours at 1800° F. X250.

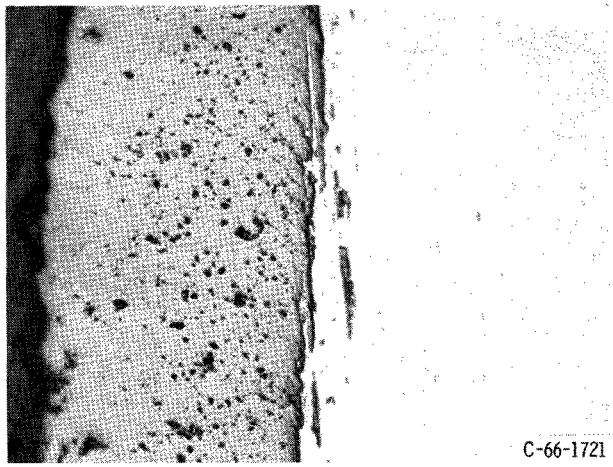

C-66-1721

(c) Tested for 1868.4 hours at 1800° F. X250.

Figure 12. - Microstructures of as-polished Ni + 2 volume percent ThO_2 after stress-rupture tests.

(a) No appreciable microporosity. X19 000.

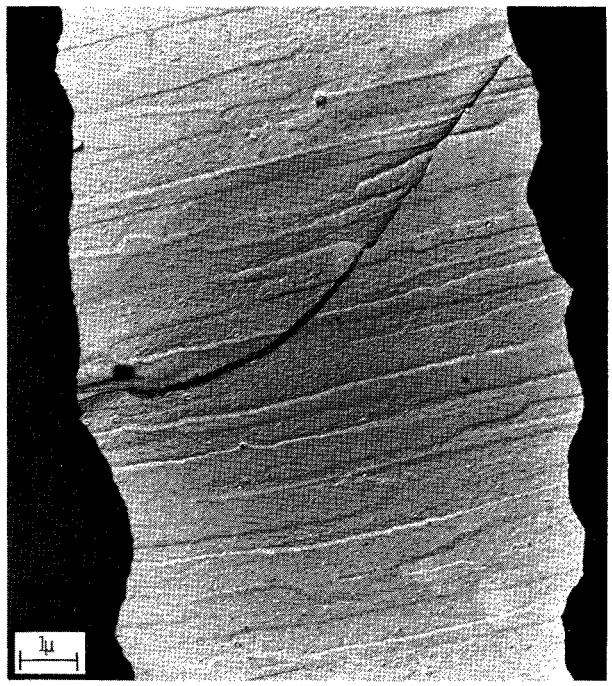

(b) No appreciable microporosity. X7000.

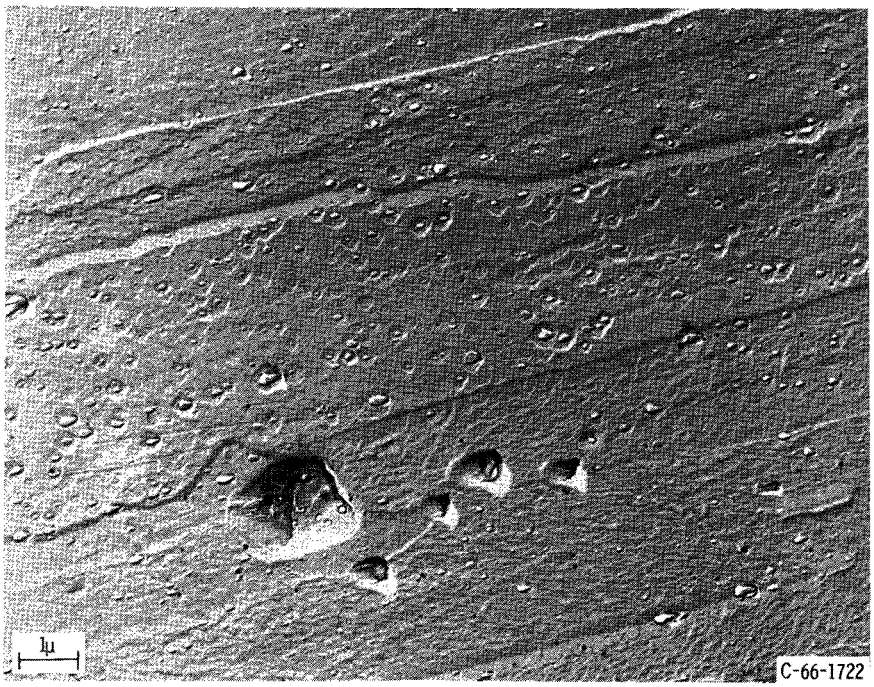

(c) Some microporosity. X19 000.

Figure 13. - Ni + 2 volume percent ThO_2 after testing in stress rupture for 1868.4 hours at 1800° F. (Note the absence of any appreciable microporosity and retention of the fine dispersoids.

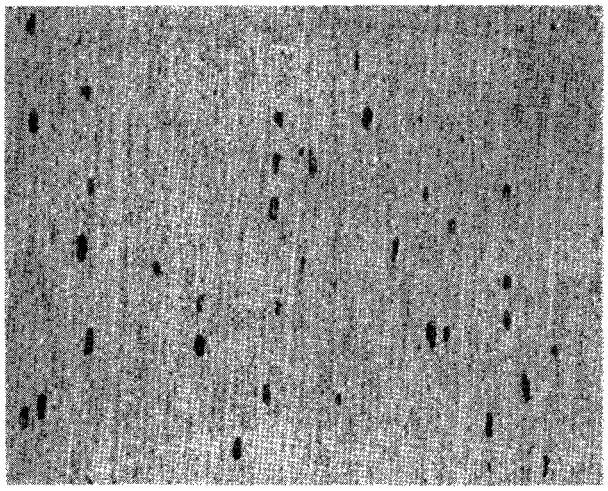

(a) Microstructure prior to post-stress-rupture thermal treatment. As polished. X750.

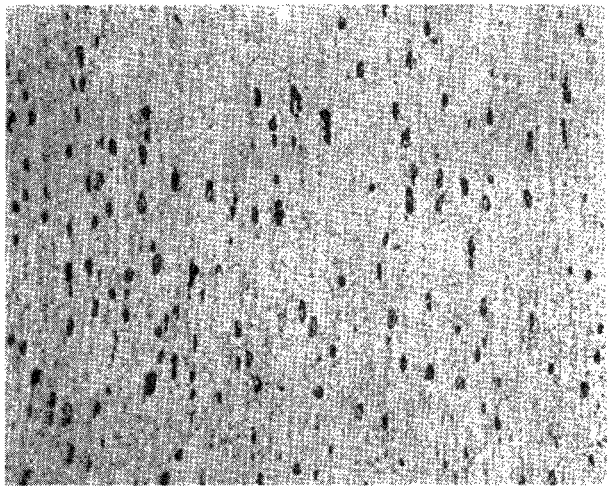

(b) Microstructure after post-stress-rupture test thermal treatment. As polished. X750.

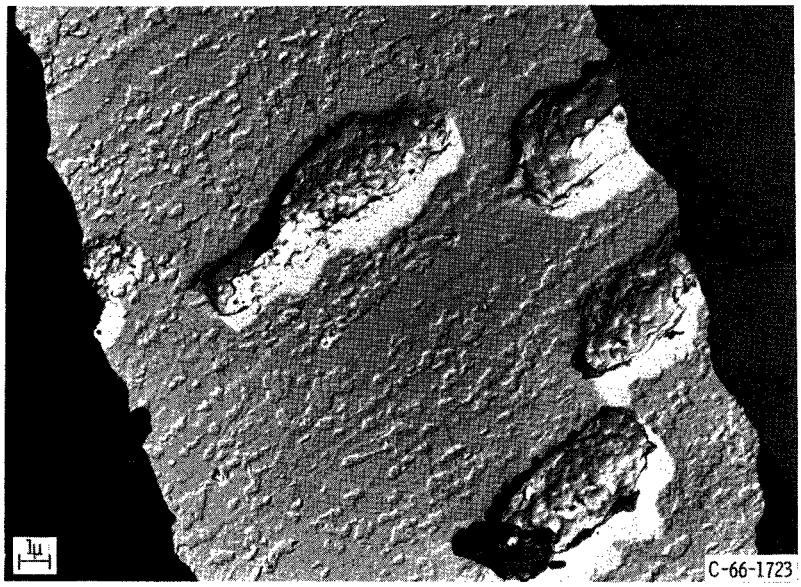

(c) Microstructure after thermal treatment. X7000. (Note voids and also that dispersoid particles have grown by comparison with fig. 11(e).)

Figure 14. - Ni + 7.5 volume percent ThO_2 initially tested in stress-rupture for 37 hours at 1500° F and subsequently heat treated for 5 hours at 2000° F in vacuum.

The electron micrographs of the specimen shown in figure 13, which had been run for 1868.4 hours at 1800° F, revealed no apparent change in microstructure and indicated good stability of both matrix and particles alike. There was no indication that the dark areas in the optical micrographs were voids, as in the nickel-base alloys containing either 7.5 or 9 volume percent ThO_2. Microcracks were detected (figs. 13(a) and (b)) at approximately 45° to the specimen axis, which indicated that fracture might be initiated by shear in these specimens.

Heat Treated Nickel Plus Thoria Alloys

Figure 14(a) shows a Ni + 7.5 volume percent ThO_2 specimen taken from the grip end of a specimen that had been run for 37 hours at 1500° F. Figure 14(b) shows this same material after heat treatment for 5 hours at 2000° F in vacuum. Much more porosity is apparent after heating than may be observed in the as stress-rupture-tested material. Figure 14(c), which is an electron micrograph of the heat treated material, shows that the

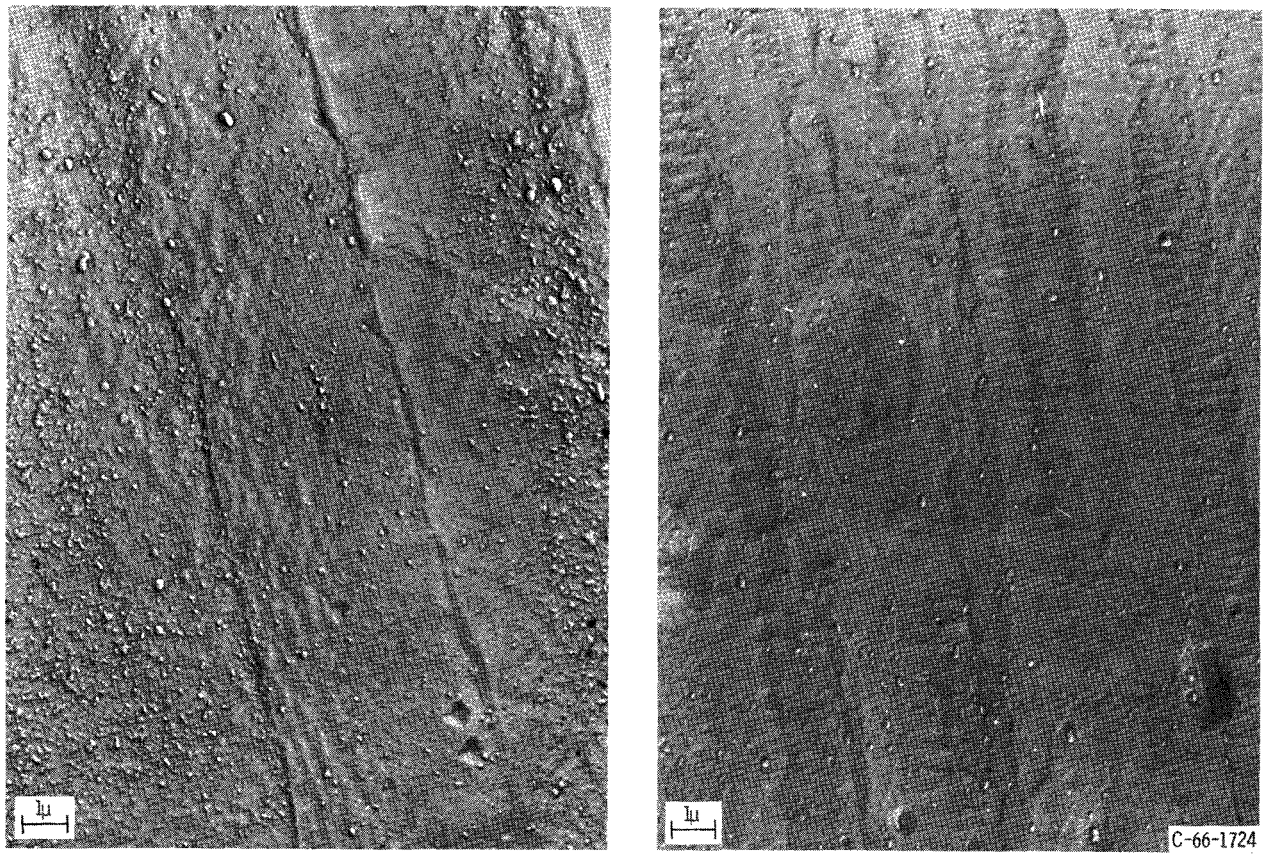

(a) As received. X12 750.

(b) Heat treated for 100 hours at 2000° F in argon. X12 750.

Figure 15. - Comparison of as-received Ni + 2 volume percent ThO_2 before and after heat treatment.

dark regions are pores, not particle agglomerates. Comparison of figures 14(c) and 11(e) (which are the same specimen) also shows that thermal treatment has caused growth of particles. Figure 15(a) is an electron micrograph of the Ni + 2 volume percent ThO_2 product (TD-Ni) in the as-received condition, and figure 15(b) represents the material after heat treatment. These electron micrographs indicate that the thermal exposure of 100 hours at 2000° F in argon did not noticeably affect the microstructure. Thermal exposure of this material has not caused oxide agglomeration or dissolution, nor does it seem to have caused porosity.

DISCUSSION

Relation Between Microstructural Stability and Stress-Rupture Properties

In general, the dispersion-strengthened alloys that exhibited the best overall retention of stress-rupture strength with increasing temperature had the most stable microstructures. The materials, Al + 5 volume percent Al_2O_3, Ni + 2 volume percent ThO_2, Cu + 3.5 volume percent Al_2O_3, and Cu + 1.1 volume percent Al_2O_3 had the best overall retention of stress-rupture strength with increasing temperature (fig. 1, p. 3). These materials also exhibited the highest overall resistance to porosity formation and/or particle agglomeration during stress-rupture testing or during thermal treatment alone (i.e., figs. 6 to 15). A further example of the microstructural stability of aluminum plus alumina is indicated in reference 8, where it is reported that SAP 930 and SAP 960 containing 7 and 4 weight percent Al_2O_3, respectively, were heated almost to the melting point of the aluminum with no deleterious effects on the microstructure.

In summary, the observation is also made that the temperatures at which the curves of stress-rupture strength as a function of homologous temperature showed an abrupt or noticeable decrease relative to the initial slopes of the curves would appear to correspond to the onset of or the accelerated rate of formation of porosity; this is so for the Ni + 7.5 and 9 volume percent ThO_2 materials and to a lesser extent for the Cu + Al_2O_3 materials. The data obtained from reference 9 for Al + 5 volume percent Al_2O_3, also show an abrupt downward change in the slope of the homologous plot (fig. 1), but a possible reason for this is not apparent unless perhaps it might be associated with temperature-dependent structural instabilities of the intermetallic particle. The Ni + 7.5 volume percent ThO_2 and Ni + 9 volume percent ThO_2 materials had very good stress-rupture strengths at lower temperatures, but lost strength relatively more rapidly at higher temperatures (i.e., above 0.73 $T/T_{M.P.}$); this more rapid drop was believed to be due to the accelerated rate of formation of microporosity at higher temperatures. As noted in figure 11, these pores might link up to cause specimen failure. The Ni + 7.5 volume percent ThO_2

developed additional, extensive porosity upon post stress-rupture test annealing at 2000° F (fig. 14).

For the copper plus alumina material, a slight, but preceptible, downward break in the slope of the homologous plots occurred at about 0.68 $T/T_{M.P.}$ (fig. 1). This slightly more rapid decrease in strength with temperature, above 0.68 $T/T_{M.P.}$ is also believed to be associated either with the onset of or the accelerated rate of formation of porosity. The overall extent of porosity appeared to be much less in the copper plus alumina materials than in the Ni + 7.5 or 9 volume percent ThO_2 materials.

Analysis of Possible Interrelations Among Microstructural Parameters, Impurities, Porosity, and Stress-Rupture Strength

Several interesting analyses may be made based on the data summarized in table VI (p. 13). For the Ni + 7.5 volume percent ThO_2 and Ni + 9 volume percent ThO_2 materials, the measured volume fractions of particles (i.e., 12 to 18 volume percent) are substantially greater than the nominal amounts of oxide; this suggests the presence of impurities in these materials. Impurity oxide particles could have been formed during processing, or possibly nitride particles could have been present as residuals from the decomposition of the thorium nitrate used to produce the thoria dispersoid particles. A further observation indicates that specimens which had been stress-rupture tested at 2000° F may have a lesser volume fraction of particles after testing than specimens which had been stress-rupture tested at 1500° F. This suggests that perhaps some of the excess particles in these two particular Ni + ThO_2 alloys dissolved at the higher exposure temperature.

For the copper plus alumina materials an apparent excess of volume percent of measured particle existed over the nominal amount of aluminum oxide for the nominally 0.4 and 1.1 volume percent Al_2O_3 alloys. Presumably these excess particles were copper oxide. In addition it may also be noted from table VI that the Cu + 0.4 volume percent Al_2O_3 material had a measured volume percent of fine particle of 4.5 percent, while the Cu + 3.5 percent Al_2O_3 material had a measured volume percent of fine particle of 2 percent. Thus, the amount of impurity particles incorporated in these three alloys was inversely proportional to the initial amount of aluminum in the respective copper plus aluminum binary alloys. As might be expected from theoretical considerations, the use of a larger amount of aluminum in the starting binary alloy would probably result in the diffusion of a lesser amount of oxygen into the interior of the binary copper plus aluminum powder particles, with the resultant formation of a lesser amount of impurity oxides. The use of a larger initial amount of aluminum might also be expected to result in the formation of a larger amount of external scale alumina, which ultimately would form the bands of coarse particles shown in figures 7 and 9.

It should be mentioned that the amounts of particles indicated in table VI for the copper plus alumina materials do not include the coarser particles in the bands. An effort was made to determine the volume fraction of coarse particles in the bands, but the distribution of the coarser particles was very heterogeneous, and it was felt that statistically reliable values would require an inordinate amount of electron microscopy. Determinations were made, however, to at least approximate the volume percent of coarser particles in the banded regions. Values of 9.9, 5.8, and 10.7 percent were obtained respectively for Cu + nominal 3.5, 1.1, and 0.4 volume percent Al_2O_3. Thus, there was no apparent correlation between the volume percent of coarse particles in the bands and the initial amount of aluminum; this lack of correlation is believed due either to the possibility that impurity oxides as well as alumina are present in the bands or to the statistical problem noted above. A final observation that may be made is that the strengths of the copper plus alumina specimens were directly related to the nominal amounts of alumina and inversely related to the measured volume percent of fine particles. Hence it would appear that the fine nonalumina particles are not the major contributors to the strength of these three particular alloys. Since porosity is apparently inversely related to the nominal amount of aluminum oxide, the ineffectiveness of the nonalumina particle might be speculated to be due, at least in part, to the increasing propensity to porosity with increasing impurity particle content.

As a matter of related interest, speculations regarding nominal against measured particles were also made for nickel plus magnesium oxide dispersion-strengthened materials (ref. 10). In reference 10, the excess of measured particle over nominal quantity of oxide additive, which was found to be the case in a number of specimens, was felt to be due to impurity "pickup" during processing.

While there was an observed association between impurity (based on a larger amount of measured particles compared with the nominal amount) and porosity, factors other than the incorporation of impurities must be considered as possible mechanisms for the formation of porosity. Other possible mechanisms, described in references 11, 12, and 13 involve the formation of voids associated with grain boundary slip, and the condensation of vacancies at inclusions.

With respect to the Ni + 2 volume percent ThO_2 material (i.e., TD-Ni) the observed and nominal amounts of oxide are considered to be in good agreement. Since this material is reported to be of high purity (data from S. T. Wlodek, General Electric Co.), little, if any, excess particle formation would be expected. For Al + 5 volume percent Al_2O_3 material, the amounts of measured fine (nonintermetallic) particles and nominal particle are in good agreement, which suggests good purity, except for the incorporation of the intermetallic phase. This phase is believed to be deleterious as will be noted subsequently, but apparently it is not responsible for the formation of gross amounts of porosity.

As noted in the RESULTS section, the interparticle spacings for all the materials in this investigation were of the same order of magnitude (i. e., 1 to 2μ). Study of the particle sizes (table V, p. 10), reveals that the more strength stable materials, which include Al + 5 volume percent Al_2O_3, Ni + 2 volume percent ThO_2, and Cu + Al_2O_3 have the finest particle sizes, being less than about 0.05 micron. (In this generalization, the thickness of the alumina particles in the aluminum plus alumina material is presumed to characterize these oxide particles and is reported to be in the 0.005 to 0.05 μ range, refs. 6 and 7.) These materials also tend to have fairly well distributed particles. (For the copper plus alumina material, this would apply to the fine background dispersion.) Thus retention of stress-rupture strength appears to be dependent on fineness of the dispersoid and perhaps to a lesser extent on the uniformity of the dispersion; these observations appear to be consistent with current dispersion-strengthening theory. With regard to the uniformity of the dispersion-strengthening particles, it is inductively obvious that relatively good uniformity is necessary. If there are regions of the material that are devoid of reinforcement, these regions obviously will be weak in comparison to the more effectively dispersion-strengthened regions; thus failure could be initiated in these weaker regions.

No evidence was obtained in this study to indicate that intentional oxide additives agglomerated during stress-rupture thereby contributing to instability. That is, there was no indication that particle coarsening occurred at higher temperatures, causing relatively more rapid losses in strength. On the other hand, there was an association between the amount of impurity particles (based upon measured against nominal amounts of particles) and the extent of porosity formation. Intentionally added particles obviously are chosen for their inherent stability and would be expected to be thermodynamically stable, unless in the presence of impurity materials or perhaps the matrix itself their thermodynamic stabilities were lessened. However, matrix oxides and/or compounds might well be less stable than the intentionally added dispersoids. Less stable particles could undergo dissolution, and thus the matrix material would no longer be dispersion strengthened. Furthermore, dissolution reactions and/or the entrapment of occluded gases which could occur during processing, could give rise to the formation of gas pockets and thus be even more damaging than dissolution.

Fracture Observations

No unique fracture mode could be associated with the stronger, more stable materials. The copper plus alumina alloys exhibited ductile fracture, while the nickel plus thoria alloys exhibited brittle fracture. The Al + 5 volume percent Al_2O_3 specimens appeared to possess ductility in shorttime stress-rupture testing, but were brittle after longtime stress-rupture testing.

Possible effects of lamellae of coarse dispersoids. - An interesting observation may be made with regard to the copper plus alumina materials. Study of the microstructures reveals that in various portions of the fractured stress-rupture specimens, zones existed that appear to have "necked down" producing in part a lateral crack (i.e., a crack perpendicular to the direction of loading) and in part a crack parallel to the lamellae of coarse particles. The crack of the necked-down portion extended from one major lamellar segregation of large particles to another. The zones between the coarse particle lamellae are speculated to be weaker than the coarse particle lamellar zones and to tend to deform, which result in both internal necking and separation at the interfaces between two zones. The coarse particle lamellar zones would have to be tougher than the intervening material. If the entire microstructure consisted of the weaker matrix containing the fine dispersoids, a crack that might form, could then propagate across a specimen with relative rapidity. Bands of larger particles are speculated as having the capability of inhibiting the rapid propagation of a crack through a specimen. This rapid crack propagation would suggest that a "lamellar" dispersion-strengthened product could have very desirable stress-rupture characteristics, as did the copper plus internally oxidized aluminum specimens and that a perfectly uniform distribution of the dispersoids throughout the material is not necessary. In fact, under some circumstances, a heterogeneous microstructure might be advisable consisting of fine uniformly distributed oxide particles and parallel lamellae of hard discrete particles somewhat larger than the particles generally present in the matrix. Such lamellae could act as crack inhibitors.

Crack initiation due to large particles in the aluminum plus 5 volume percent aluminum oxide material. - Observation of the Al + 5 volume percent Al_2O_3 specimens, regardless of their test duration, revealed the presence of voids adjacent to or cracks within the $FeAl_3$ intermetallic particles. These particles were estimated to be about 25 microns in size, several orders of magnitude larger than the thickness of the dispersion-strengthening alumina particles. According to reference 4, large $FeAl_3$ intermetallic particles are recognized as being capable of introducing stress-concentrations in aluminum (sintered aluminum powder). It is apparent that while the fine alumina particles can act as dislocation barriers, the much coarser $FeAl_3$ particles can induce adjacent void formation and/or completely fracture and cause crack propagation into the matrix. This effect is opposite to that shown previously when smaller but still relatively coarse particles in lamellar arrangements appeared beneficial to the copper plus alumina alloys.

CONCLUSIONS

A metallographic study was conducted on a number of dispersion-strengthened materials to obtain additional insight into the microstructural factors affecting their stress-

rupture strengths. This study led to the following conclusions:

1. In general, the dispersion-strengthened alloys investigated herein that exhibited the best overall retention of stress-rupture strength with increasing temperature also had the most stable microstructures; that is, these alloys had a superior resistance to porosity formation in stress-rupture and in thermal treatment. They also appeared more resistant to particle coarsening in thermal treatment alone.

2. Those materials that had measured amounts of particles appreciably beyond the nominal amounts of intentionally added oxide had good stress-rupture properties at lower temperatures; however, at higher temperatures, their stress-rupture strengths decreased relatively more rapidly. The more rapid rate of stress-rupture strength loss at higher temperature was believed associated with the formation of porosity.

3. Porosity was believed to result from impurity reactions and/or gas entrapment. Impurities and concurrent porosity presumably were more damaging to materials at higher test temperatures than at lower test temperatures. Thus, dispersion-strengthened materials may probably tolerate impurities and even some porosity at lower test temperatures, but at high temperatures impurity reactions may be extremely damaging. It would then follow that to achieve its full potential strength a dispersion-strengthened material should contain a minimal impurity content.

4. There was no unique fracture mode that could be associated with the stronger more stable materials.

5. The best retention of stress-rupture strength with increasing temperature was associated with fine (i. e., whose characterizing dimension was less than about 0.05 μ) and uniformly distributed background dispersoid particles.

6. Large particles, such as the $FeAl_3$ inclusions in the Al + 5 volume percent Al_2O_3 alloy can cause deleterious void or crack formations. Conversely, however, copper plus alumina dispersion-strengthened materials may have been benefited by the presence of lamellar bands of somewhat larger particles than those embedded in the matrix.

Lewis Research Center,
National Aeronautics and Space Administration,
Cleveland, Ohio, March 15, 1966.

REFERENCES

1. Irmann, R.: Sintered aluminum with High Strength at Elevated Temperature. Metallurgia, vol. 46, no. 275, Sept. 1952, pp. 125-133.

2. Cremens, Walter S.: Use of Submicron Metal and Nonmetal Powders for Dispersion-Strengthened Alloys. Ultrafine Particles, W. E. Kuhn, ed., John Wiley & Sons, Inc., 1963, pp. 457-478.

3. Smith, Cyril Stanley; and Guttman, Lester: Measurement of Internal Boundaries in Three Dimensional Structures by Random Sectioning. AIMME Trans., J. Metals, vol. 197, no. 1, Jan. 1953, pp. 81-87.

4. Hess, E. G.: Einfluss Unterschiedlicher Kalterformungen Auf die Mechanischen Eigen-Schaften und den Dispersionsgrad von Sinteraluminium. Z. Metallk., vol. 55, no. 3, 1964, pp. 123-127.

5. Theisen, R.: Anwendung des Rontgenmikroanalysators zur Untersuchung des Zéilengefuges von Kaltverformtem Sinteraluminium. Z. Metallk., vol. 55, no. 3, 1964, pp. 128-134.

6. Bloch, E. A.: Dispersion-Strengthened Aluminum Alloys. Met. Rev., vol. 6, no. 22, 1961, pp. 193-239.

7. Bollenrath, F.: Sintered Aluminum S. A. P. Rept. No. 103, AGARD, Apr. 1957.

8. Brammar, I. S.; and Dawe, D. W.: Metallography of S. A. P. Alloys and Its Relation to Creep Resistance. (AFML TDR-64-211, DDC No. AD-608868), Aeon Labs. (Egham, Great Britain), Oct. 1964.

9. Preston, Oliver; and Grant, Nicholas J.: Dispersion Strengthening of Copper by Internal Oxidation. AIME Trans., vol. 221, no. 1, Feb. 1961, pp. 164-173.

10. Schafer, Robert J.; Quatinetz, Max; and Weeton, John W.: Strength and High-Temperature Stability of Dispersion Strengthened Nickel-MgO Alloys. AIME Trans., vol. 221, Dec. 1961, pp. 1099-1104.

11. Cottrell, A. H.: Theoretical Aspects of Fracture. Fracture; Proceedings of an International Conference on the Atomic Mechanism of Fracture, B. L. Averbach, D. K. Felback, G. T. Hahn, and D. A. Thomas, eds., Technology Press of MIT and John Wiley & Sons, Inc., 1959, pp. 20-53.

12. Davies, P. W.; and Dennison, J. P.: A Review of Intergranular Fracture Processes in Creep. J. Inst. Metals, vol. 87, 1958-1959, pp. 119-125.

13. Resnick, R.; and Seigle, L.: Nucleation of Voids in Metals During Diffusion and Creep. J. Metals, vol. 9, Jan. 1957, pp. 87-94.

14. Anon.: DuPont TD Nickel Dispersion Strengthened Nickel. DuPont Metal Products, New Products Information. DuPont Metals Center (Baltimore).

15. Murphy, Richard; and Grant, Nicholas J.: Properties of Nickel-Thoria Alloys Prepared by Thermal Decomposition of Thorium Nitrate. Powder Met., no. 10, 1962, pp. 1-12.

16. Predecki, Pawel; and Grant, Nicholas J.: Oxide Refractories in Dispersion-Strengthened Copper and Nickel Alloys. Prep. No. 66, ASTM, 1962.

17. Guy, Dan M., Jr.: Alcoa's Aluminum Powder Metallurgy (APM) Alloys. Alcoa Green Letter No. 165, Alcoa, Mar. 1959.

18. Gregory, Eric; and Grant, Nicholas J.: High Temperature Strength of Wrought Aluminum Powder Products. Dept. of Metallurgy, MIT, 1954.

19. Bieber, C. G.; and Kihlgren, T. E.: A New Cast Alloy for Use at 1900° F. Metal Progr., vol. 79, no. 4, Apr. 1961, pp. 97-99.

NASA-Langley, 1966 E-2982

"The aeronautical and space activities of the United States shall be conducted so as to contribute . . . to the expansion of human knowledge of phenomena in the atmosphere and space. The Administration shall provide for the widest practicable and appropriate dissemination of information concerning its activities and the results thereof."

—NATIONAL AERONAUTICS AND SPACE ACT OF 1958

NASA SCIENTIFIC AND TECHNICAL PUBLICATIONS

TECHNICAL REPORTS: Scientific and technical information considered important, complete, and a lasting contribution to existing knowledge.

TECHNICAL NOTES: Information less broad in scope but nevertheless of importance as a contribution to existing knowledge.

TECHNICAL MEMORANDUMS: Information receiving limited distribution because of preliminary data, security classification, or other reasons.

CONTRACTOR REPORTS: Technical information generated in connection with a NASA contract or grant and released under NASA auspices.

TECHNICAL TRANSLATIONS: Information published in a foreign language considered to merit NASA distribution in English.

TECHNICAL REPRINTS: Information derived from NASA activities and initially published in the form of journal articles.

SPECIAL PUBLICATIONS: Information derived from or of value to NASA activities but not necessarily reporting the results of individual NASA-programmed scientific efforts. Publications include conference proceedings, monographs, data compilations, handbooks, sourcebooks, and special bibliographies.

Details on the availability of these publications may be obtained from:

SCIENTIFIC AND TECHNICAL INFORMATION DIVISION

NATIONAL AERONAUTICS AND SPACE ADMINISTRATION

Washington, D.C. 20546